BIOCHEMISTRY
including biophysical chemistry & molecular biology
Article

Biochemistry **2010,** *49,* 5671–5682 5671
DOI: 10.1021/bi9019498

Recognition of Galactose-Deficient *O*-Glycans in the Hinge Region of IgA1 by *N*-Acetylgalactosamine-Specific Snail Lectins: A Comparative Binding Study[†]

Michelle M. Gomes,[‡,@] Hitoshi Suzuki,[§,⊥,#] Monica T. Brooks,[‡,#] Milan Tomana,[∥] Zina Moldoveanu,[§] Jiri Mestecky,[§,∥] Bruce A. Julian,[§,∥] Jan Novak,[§] and Andrew B. Herr*[,‡]

[‡]*Department of Molecular Genetics, Biochemistry and Microbiology, University of Cincinnati College of Medicine, Cincinnati, Ohio 45267-0524,* [§]*Department of Microbiology, and* [∥]*Department of Medicine, University of Alabama at Birmingham, Birmingham, Alabama 35294, and* [⊥]*Department of Nephrology, Juntendo University School of Medicine, Tokyo, Japan* [@]*Current address: Molecular and Computational Biology, University of Southern California, Los Angeles, CA 90089-2910.*
[#]*These authors contributed equally to this work.*

Received November 11, 2009; Revised Manuscript Received May 27, 2010

ABSTRACT: Aberrancies in IgA1 glycosylation have been linked to the pathogenesis of IgA nephropathy (IgAN), a kidney disease characterized by deposits of IgA1-containing immune complexes in the glomerular mesangium. IgA1 from IgAN patients is characterized by the presence of galactose (Gal)-deficient *O*-glycans in the hinge region that can act as epitopes for anti-glycan IgG or IgA1 antibodies. The resulting circulating immune complexes are trapped in the glomerular mesangium of the kidney where they trigger localized inflammatory responses by activating mesangial cells. Certain lectins recognize the terminal *N*-acetylgalactosamine (GalNAc)-containing *O*-glycans on Gal-deficient IgA1 and can be potentially used as diagnostic tools. To improve our understanding of GalNAc recognition by these lectins, we have conducted binding studies to assess the interaction of *Helix aspersa* agglutinin (HAA) and *Helix pomatia* agglutinin (HPA) with Gal-deficient IgA1. Surface plasmon resonance spectroscopy revealed that both HAA and HPA bind to a Gal-deficient synthetic hinge region glycopeptide (HR-GalNAc) as well as various aberrantly glycosylated IgA1 myeloma proteins. Despite having six binding sites, both HAA and HPA bind IgA1 in a functionally bivalent manner, with the apparent affinity for IgA1 related to the number of exposed GalNAc groups in the IgA1 hinge. Finally, HAA and HPA were shown to discriminate very effectively between the IgA1 secreted by cell lines derived from peripheral blood cells of patients with IgAN and that from cells of healthy controls. These studies provide insight into lectin recognition of the Gal-deficient IgA1 hinge region and lay the groundwork for the development of reliable diagnostic tools for IgAN.

Abnormalities in IgA1[1] glycosylation have been implicated in several diseases such as Sjögren's syndrome (*1*), Henoch-Schönlein purpura nephritis, and IgA nephropathy (IgAN) (*2*−*12*). Human IgA1 is one of only a few serum proteins that contain both *N*- and *O*-linked glycans (*13*−*18*). There are up to six *O*-glycans on each heavy chain of IgA1, each linked to a Ser or Thr residue in the hinge region between the C_H1 and the C_H2 domains (*13*, *19*−*26*). Each *O*-glycan consists of a core *N*-acetylgalactosamine (GalNAc) typically linked to galactose (Gal) and one or two sialic acid residues, giving rise to six *O*-glycan variants (Figure 1) (*13*, *20*−*22*, *27*). It is well established that patients with IgAN have abnormalities in *O*-glycan biosynthesis resulting in the exposure of the core GalNAc residue with or without sialylation (*5*, *7*, *9*, *28*−*32*); this exposed GalNAc appears to play a role in the pathogenesis of the disease. The Gal-deficient hinge region of IgA1 with terminally exposed GalNAc residue(s) is recognized by IgG or IgA1 antibodies, leading to the formation of large circulating immune complexes (CICs) that deposit in the kidney (*7*, *8*, *33*−*37*). Glomerular deposition of these CICs activates complement via the alternative (*38*, *39*) or mannose-binding lectin pathways (*40*, *41*).

Lectins are plant or animal proteins that recognize specific carbohydrate groups and therefore have been used to study protein glycosylation in many disease states, including cancer (*42*−*44*) and chronic inflammatory diseases (*30*, *44*−*49*). Furthermore, GalNAc-specific lectins, such as *Helix aspersa* agglutinin (HAA) and *Helix pomatia* agglutinin (HPA), derived from garden and edible roman snails, respectively, have been used to study the *O*-glycosylation of IgA1 from patients with IgAN or multiple myeloma (*2*, *3*, *7*−*9*, *28*, *30*, *48*, *50*). The X-ray crystal structure of HPA showed that it is a hexamer formed by disulfide-linked dimers of noncovalent trimers (*51*), with GalNAc-binding sites at the end of each trimer, in the interface between subunits. The dissociation constant for GalNAc binding

[†]This research was supported by National Institutes of Health Grants DK071802, DK078244, DK080301, DK082753, DK075868, DK077279, DK064400, and DK061525, funds from the Ohio Eminent Scholar Program, and the Center for Clinical and Translational Sciences of the University of Alabama at Birmingham (1UL1RR025777).

*To whom correspondence should be addressed. E-mail: Andrew.Herr@UC.edu. Phone: (513) 558-5312. Fax: (513) 558-1190.

[1]Abbreviations: IgA1, immunoglobulin A1; IgAN, IgA nephropathy; Gal, galactose; GalNAc, *N*-acetylgalactosamine; HAA, *Helix aspersa* agglutinin; HPA, *Helix pomatia* agglutinin; HR, hinge region; CIC, circulating immune complex; ELISA, enzyme-linked immunosorbent assay; EBV, Epstein-Barr virus; SDS−PAGE, sodium dodecyl sulfate−polyacrylamide gel electrophoresis; PVDF, polyvinyl difluoride; Fab, antigen-binding fragment; AUC, analytical ultracentrifugation; SPR, surface plasmon resonance; NHS, *N*-hydroxysuccinimide; EDC, 1-ethyl-3-[3-(dimethylamino)propyl]carbodiimide hydrochloride; HBS, Hepes-buffered saline; PDEA, 2-(2-pyridinyldithio)ethaneamine; TBS, Tris-buffered saline; RU, response units; FT-ICR, Fourier transform ion cyclotron resonance; Fc, crystallizable fragment.

Published on Web 05/27/2010

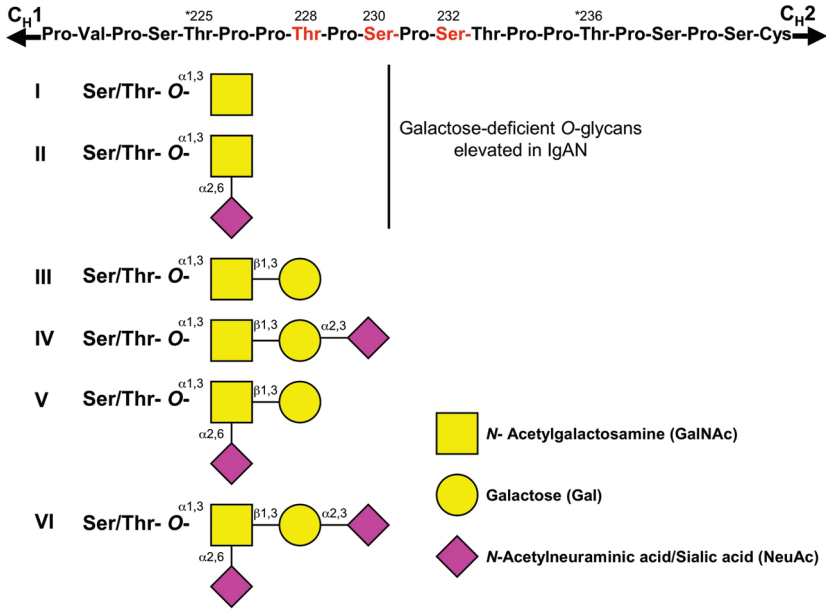

FIGURE 1: *O*-Linked glycans in the hinge region of circulatory IgA1. Potential sites of *O*-glycan attachment are numbered (*22*); red denotes sites of GalNAc attachment in the HR−GalNAc synthetic hinge peptide. *N*-Acetylgalactosamine (GalNAc) is attached by a glycosidic *O*-linked bond to serine (Ser) or threonine (Thr) residues in the hinge region of IgA1 to form the Tn antigen (**I**). Galactose (Gal) is attached to GalNAc by a *β*-1,3-linked glycosidic bond, forming the core 1 structure (**III**) that, in turn, can be sialylated with one or two *N*-acetylneuraminic acid (NeuAc) residues to form structures **IV**, **V**, and **VI**. The configuration in structure **II** is a sialylated Tn antigen that, along with the Tn antigen, is commonly seen in IgAN patients in elevated amounts.

to HPA has been reported to be 130 μM by isothermal titration calorimetry (*51*). Although HAA has been the best lectin for recognizing the glycosylation of IgA1 from IgAN patients (*3*, *48*), detailed biochemical characterization of this lectin is lacking. In this study, we demonstrated by analytical ultracentrifugation (AUC) and a competition-based biosensor assay that HAA, like HPA, exists mainly as a hexamer in solution and can bind individual GalNAc residues with an affinity in the high micromolar range. Previous studies have used HAA and HPA in ELISA and Western blotting to study aberrancy in glycosylation of IgA1 molecules (*3*, *6*, *7*, *9*, *28*, *30*, *48*, *50*). To study the interaction in real time and to help unravel the mechanism of binding, we have used surface plasmon resonance (SPR) spectroscopy to determine the affinities and specificities of HAA and HPA for various IgA1 myeloma proteins and IgA1 secreted by IgA1-producing cell lines originating from IgAN patients and healthy controls. Our studies showed that the GalNAc-specific lectins had the highest affinity for $IgA1_{Ale}$ and that the lectins bound much more tightly to IgA1 from IgAN patients than to IgA1 from healthy controls. On the basis of these studies, we suggest that a lectin-based sensor chip assay can be used in the diagnosis and/or screening of IgAN, assuming that the aberrantly glycosylated hinge region of IgA1 is a marker for the disease.

EXPERIMENTAL PROCEDURES

Reagents. Native and biotinylated HAA (Sigma-Aldrich) and HPA (EY Laboratories) were used for binding assays and lectin Western blotting, respectively. *Sambucus nigra* agglutinin (SNA, specific for α-2,6-linked sialic acid) and *Maackia amurensis* agglutinin II (MAA-II, specific for α-2,3-linked sialic acid) were purchased from Vector Laboratories and used for binding assays as well. Myeloma patient-derived IgA1*κ* and IgA1*λ* proteins were obtained from Biodesign International (Cincinnati, OH); $IgA1_{Mce}$ and $IgA1_{Ale}$ are myeloma patient-derived proteins that have been previously described (*8*, *9*, *18*, *37*). Each IgA1 sample was further purified by size-exclusion chromatography using a Hi Load 16/60 Superdex 200 column (GE Healthcare) into monomeric and polymeric fractions. Size-exclusion chromatography-purified monomeric IgA1 (termed mIgA1*κ*, mIgA1*λ*, $mIgA1_{Mce}$, and $mIgA1_{Ale}$) and polymeric IgA1 fractions (termed pIgA1*κ*, pIgA1*λ*, $pIgA1_{Mce}$, and $pIgA1_{Ale}$) were used for binding experiments. IgA1 proteins from IgAN patients and healthy controls were purified from culture media from EBV-immortalized IgA1-secreting cells originating from peripheral blood cells from patients with IgAN and from healthy controls, as previously described (*9*). The *O*-glycans of IgA1 secreted from cells of IgAN patients were Gal-deficient, while IgA1 from healthy controls was normally glycosylated (*9*).

Hinge-Region Glycopeptide (*HR-GalNAc*). A glycopeptide with GalNAc residues attached at three sites frequently observed in the hinge region of IgA1 in IgAN patients (HR-GalNAc) (*52*) was synthesized by Bachem (Torrance, CA); HR-GalNAc is composed of 20 amino acids of the IgA1 hinge region (VPSTPP**T**P**S**P**S**TPPTPSPSC), with GalNAc residues attached at positions 228, 230, and 232 (bold and underlined) (*9*, *37*).

Lectin Western Blots. IgA1 myeloma proteins or IgA1 secreted from EBV-immortalized B cells from IgAN patients and healthy controls (0.5 μg) were electrophoretically separated by reducing SDS−PAGE and transferred to polyvinyl difluoride membranes (PVDF) for antibody and lectin binding (*9*, *37*). Briefly, for lectin blots, the membrane was blocked with Superblock (Pierce, Rockford, IL), followed by incubation with biotinylated HAA or HPA. After being washed, the membrane was incubated with horseradish peroxidase-conjugated NeutrAvidin (Pierce). Detection was conducted using SuperSignal (Pierce). For Western blot detection of IgA, the membrane was blocked with Superblock (Pierce) and washed, followed by incubation with the biotinylated $(Fab')_2$ fragment of goat anti-human IgA1 heavy chain-specific antibody (Vector, Burlingame, CA) and developed with horseradish peroxidase-conjugated NeutrAvidin (Pierce)

followed by enhanced chemiluminescent detection (SuperSignal, Pierce).

Analytical Ultracentrifugation (*AUC*). Sedimentation velocity and equilibrium experiments were conducted in a Beckman XL-I ProteomeLab analytical ultracentrifuge using absorbance optics. For sedimentation velocity experiments, 3.7 μM HAA or HPA in TBS [20 mM Tris-HCl (pH 7.4) and 150 mM NaCl] was loaded into two-sector centerpieces and spun at 36000 rpm and 20 °C. Data were analyzed using $c(s)$ and $c(M)$ models in SEDFIT (*53*) to determine differential sedimentation coefficient and apparent mass distributions, respectively. To determine the assembly state, sedimentation equilibrium experiments were conducted at 20 °C at rotor speeds of 10000, 14000, 17000, and 24000 rpm. HAA or HPA solutions (100 μL) at concentrations ranging from 0.353 to 2 μM were loaded into six-channel centerpieces. Radial scans at 230 and 280 nm were collected as the average of eight replicates. Data were trimmed using WinREEDIT and globally fitted using WinNONLIN (http://www.rasmb.bbri.org/). The data were fitted initially to a single-exponential curve to determine σ_w, the weight-average buoyant molecular weight, which corresponded approximately to a hexamer. A hexamer−dodecamer assembly model did not result in an improvement of the fit for HAA or HPA; each lectin existed only as a hexamer at the concentrations used in the equilibrium experiments. The partial specific volume of HPA, calculated on the basis of its amino acid sequence, was 0.7270 mL/g, and buffer density was calculated as 1.00499 g/mL using SEDNTERP (*54*). Although the entire amino acid sequence of HAA is unknown, preliminary mass spectrometry analysis indicates a high degree of sequence similarity to HPA (M. M. Gomes, K. D. Greis, and A. B. Herr, unpublished observations); thus, the partial specific volume of HPA was used as a close approximation. Calculation of experimental molecular weights from σ_w was performed as described previously (*55*, *56*).

Biosensor Analyses. Surface plasmon resonance (SPR) biosensor assays were conducted on a Biacore 3000 instrument (GE Healthcare) at 25 °C. For immobilization of the HR-GalNAc glycopeptide, thiol coupling chemistry was used as described in Biacore Application Note 9. Briefly, the surface of a CM5 chip was activated using a 1:1 mixture of *N*-hydroxysuccinimide (NHS) and 1-ethyl-3-[3-(dimethylamino)propyl]carbodiimide hydrochloride (EDC) at a flow rate of 5 μL/min with HBS-P [20 mM HEPES (pH 7.4), 150 mM NaCl, and 0.005% P-20] as the running buffer. Reactive disulfides were introduced using 2-(2-pyridinyldithio)ethaneamine (PDEA), followed by injection of 50 μg of the glycopeptide per milliliter in 10 mM sodium acetate buffer (pH 4.5) until 194 and 80 RU were coupled in flow cells 3 and 4, respectively (1 RU corresponds to 1 pg of protein coupled per square millimeter on the chip). Excess reactive groups were inactivated using 50 mM cysteine and 1 M NaCl. Equilibrium binding experiments were conducted via injection of HAA or HPA in TBS-P [20 mM Tris-HCl (pH 7.4), 150 mM NaCl, and 0.005% P-20] at a flow rate of 5 μL/min for 25 min and at concentrations ranging from 50 μM to 0.28 nM. The chip surface was regenerated by three consecutive injections of 20 μL of 10 mM glycine-HCl (pH 2.0). Raw data were trimmed using BIAevaluation version 3.1. The equilibrium response (R_{eq}) at each injected lectin (analyte) concentration was averaged over 60 s using Scrubber version 2 (BioLogic Software, Campbell, Australia), and the data from both flow cells were globally fitted to an equation describing a two-site model in Scientist (Micromath Scientific Software, Salt Lake City, UT), as described previously (*18*, *55*). The total response at the plateau of each binding curve for each concentration of HAA or HPA injected was plotted versus the logarithm of the lectin concentration to yield equilibrium binding isotherms. Single-site binding models could not adequately describe the HAA or HPA data (see Figure S1 of the Supporting Information); the raw data described binding isotherms that were much more shallow than those described by a single-site binding event. Initial attempts at kinetic analysis of these binding data revealed that none of the potential binding models was able to adequately describe the association and dissociation phases of the raw binding data, presumably because of the multivalent nature of the analyte. Thus, equilibrium data were collected using a flow rate of 5 μL/min.

To determine the binding affinity of the lectin for a single GalNAc group, we conducted a biosensor-based competition assay. For the competition assay, HAA or HPA was coupled to the chip at 200 or 205 RU, respectively, and 8 μM mIgA1κ was co-injected with varying concentrations of GalNAc (1, 10, 50, 100, 150, 300, and 900 μM) at a flow rate of 30 μL/min. The equilibrium response at the plateau of each curve was averaged over 60 s and plotted as a function of GalNAc concentration. The data were fitted to determine the IC_{50} using the following equation:

$$B_{obs} = \frac{\text{total} - \text{nonspecific}}{1 + [\text{GalNAc}]/IC_{50}}$$

For binding experiments with IgA1 myeloma proteins and HAA or HPA, the IgA1 myeloma proteins were used as ligands (i.e., coupled to the chip) and HAA or HPA was used as the injected analyte. Briefly, 20 μg/mL monomeric (mIgA1κ, mIgA1λ, $mIgA1_{Mce}$, or $mIgA1_{Ale}$) or polymeric (pIgA1κ, pIgA1λ, $pIgA1_{Mce}$, or $pIgA1_{Ale}$) IgA1 proteins were diluted in 10 mM sodium acetate buffer (pH 4.5) and immobilized on a CM5 sensor chip by random amine coupling chemistry until 400−414 RU immobilized protein was achieved (*18*). HAA or HPA was injected as a 3-fold dilution series at concentrations ranging from 50 μM to 2.5 nM at 30 μL/min for equilibrium binding analyses. Control experiments were also conducted by immobilization of HAA and HPA at 200−205 RU and injection of mIgA1κ, mIgA1λ, or $mIgA1_{Ale}$ at concentrations ranging from 12 μM to 1.8 nM. As seen for the HR-GalNAc−lectin interactions, the data for the binding of HAA and HPA to the myeloma IgA1 proteins could not be adequately described by a single-site binding equation; the raw data consistently formed shallow isotherms, which is consistent with the existence of at least two sites of differing affinities (Figure S2 of the Supporting Information).

For lectin binding experiments using IgA1 produced by EBV-immortalized IgA1-secreting cells, the IgA1 purified from cell culture media from cells from IgAN patients or from healthy controls was immobilized on the sensor chip at 400−413 RU by random amine coupling chemistry as described previously, and HAA or HPA was injected at concentrations ranging from 50 μM to 2.5 nM. SNA or MAA-II was injected at concentrations ranging from 16.5 μM to 0.8 nM or from 14 μM to 0.7 nM, respectively. Experiments were conducted at a flow rate of 5 or 30 μL/min in TBS-P buffer. MAA-II experiments were conducted in 10 mM Hepes (pH 7.5), 150 mM NaCl, 0.1 mM $CaCl_2$, and 0.005% P-20. In all SPR experiments, the first flow cell was mock-coupled and the response from this cell was subtracted from that for all other flow cells, followed by subtraction of the response with a buffer blank injection. Representative raw

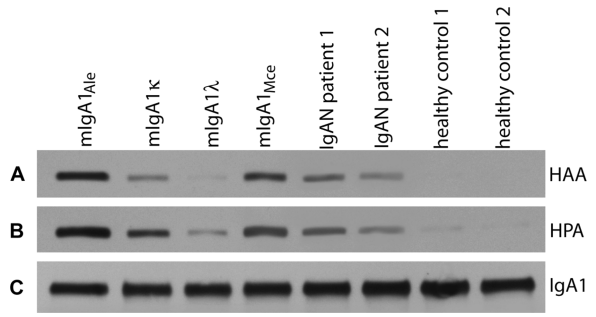

FIGURE 2: Analysis of different IgA1 proteins by lectin Western blotting. Samples of IgA1 (different IgA1 myeloma proteins and IgA1 isolated from culture supernatants of IgA1-secreting cells from the blood of IgAN patients and healthy controls) were separated by SDS−PAGE, blotted, and developed with (A) HAA, (B) HPA, or (C) IgA-specific antibody. HAA and HPA blots detect GalNAc epitopes on the IgA1 samples, and the anti-IgA1 Western blot served as a loading control.

sensorgram data for each of the binding experiments are shown in Figure S3 of the Supporting Information; in each case, HAA is shown binding to various different samples of HR-GalNAc, myeloma IgA1 proteins, or a patient-derived IgA1. Panel F of Figure S3 shows raw data for SNA binding to a patient-derived IgA1. For HAA, HPA, and SNA, the data were best described using a two-site binding model; however, a single-site binding model was appropriate for the MAA-II data. Of the data reported here, the binding of HAA and HPA to HR-GalNAc was analyzed by global analysis of two data sets at different coupling densities; other binding data were collected and analyzed as single data sets (i.e., without replicates) because of the high precision of the SPR measurements.

RESULTS

Qualitative Characterization of Binding of Lectins to Gal-Deficient IgA1. IgA1 *O*-glycans from patients with IgAN contain more terminal GalNAc residues, also called Tn antigen (GalNAc-Ser/Thr), than the IgA1 *O*-glycans from control subjects (*3*, *5*, *7*, *8*, *28*, *57*, *58*). On the basis of the fact that terminal GalNAc can be detected by specific lectins, including HAA and HPA (*2*, *3*, *6*−*9*, *28*, *30*, *48*, *50*), and that IgA1 myeloma proteins show heterogeneity in the *O*-glycans (*23*, *24*, *26*), we investigated qualitatively the levels of exposed GalNAc on various IgA1 myeloma proteins by lectin recognition on Western blots. Among the analyzed IgA1 myeloma proteins, both HAA and HPA exhibited the strongest signal with $IgA1_{Ale}$ (Figure 2). Furthermore, the IgA1 produced by the IgA1-secreting cells from IgAN patients bound more strongly to both HAA and HPA than did the IgA1 synthesized by the IgA1-secreting cells from healthy controls, consistent with prior data (*48*). These results confirmed that these lectins can be used for detection of this IgAN-specific biomarker (*3*, *7*, *9*, *48*).

Characterization of the Oligomeric State of HAA and HPA by Analytical Ultracentrifugation. Although both HPA and HAA are of interest for potential diagnosis of IgAN and are thought to have similar properties, there is currently no structural or sequence information for HAA. To establish the similarities and differences between these lectins, we compared the hydrodynamic parameters of HAA and HPA in solution by sedimentation velocity and sedimentation equilibrium experiments using an analytical ultracentrifuge. In sedimentation velocity experiments, HAA and HPA each yielded a single dominant species with sedimentation coefficients of 4.8 and 4.7 S and estimated molecular masses of ~86.8 and ~77.9 kDa, respectively (Figure 3A,B). The calculated monomeric molecular mass of HPA based on its amino acid sequence is 11326.8 Da, and HPA is *N*-glycosylated, contributing an additional 1172 Da per *N*-glycan (*51*). Thus, the AUC data suggest that both lectins exist mainly as hexamers. This result is consistent with previous X-ray structures of HPA that revealed a hexamer formed by back-to-back disulfide-linked association of two trimers (*51*). Our sedimentation data revealed that each lectin sample contained a small amount of putative dodecamer, corresponding to a sedimentation coefficient of 7.7 S for HAA and 7.3 S for HPA with estimated molecular masses of ~171 and ~150 kDa, respectively. The oligomeric state of HAA and HPA was further confirmed by sedimentation equilibrium experiments. The experimental molecular mass of HAA was calculated to be 81102 Da (76240−85950 Da), while that of HPA was 86690 Da (82708−90671 Da), confirming that both lectins exist as hexamers in solution (Figure 3C,D). At the concentrations used for sedimentation equilibrium, only the hexamer was detected, although our sedimentation velocity data suggested the presence of small amounts of dodecamer in samples with both lectins at higher concentrations.

Solution Affinity of Lectins for GalNAc Determined by an SPR Competition Assay. The crystal structure of HPA in complex with GalNAc showed that each of six sites within the HPA hexamer is capable of binding a single GalNAc molecule. Binding studies indicated that the affinity of HPA for a single GalNAc is 130 μM (*51*). To compare the affinities of HAA and HPA for GalNAc in solution, we used a biosensor competition assay. The half-maximal inhibitory concentrations (IC_{50}) for GalNAc-mediated inhibition of lectin binding to mIgA1κ were 81 ± 8 and 220 ± 20 μM for HAA and HPA, respectively (Figure 4). These IC_{50} values are comparable to the reported 130 μM affinity of HPA for GalNAc determined in isothermal calorimetry experiments (*51*).

SPR Analysis of Lectin Binding to the Gal-Deficient Hinge Region Glycopeptide. Given the importance of accurately detecting Gal-deficient IgA1 in sera and renal biopsies of patients with IgAN and the potential of lectins for this purpose, we analyzed the binding of HAA and HPA to a synthetic glycopeptide (HR-GalNAc) corresponding to the IgA1 hinge region with three GalNAc residues at T228, S230, and S232. This HR-GalNAc glycopeptide is relevant because it resembles the major antigenic epitopes in IgAN patients. Binding curves were generated by injection of HAA or HPA over HR-GalNAc coupled to a Biacore sensor chip. The data could not be satisfactorily fitted by a single-site binding equation but were described quite well by a two-site model, yielding apparent affinities significantly higher than the single-site affinity for individual GalNAc binding (i.e., 130 μM). Global fits of data sets collected from two flow cells coupled at different glycopeptide densities yielded apparent affinities of HAA and HPA for the glycopeptide of 0.11 ± 0.01 and 0.0448 ± 0.006 μM for the first binding event and 7 ± 2 and 2.3 ± 0.6 μM for the second binding event, respectively (Figure 5 and Table 1). The higher apparent affinity of each lectin for HR-GalNAc compared to that for a single GalNAc molecule is expected, because of the multivalent nature of the lectins. In this experimental orientation, the multivalent lectins were injected over the HR-GalNAc-coupled chip, resulting in a range of multivalent binding modes. Because of the small size of the HR-GalNAc glycopeptide, its coupling density

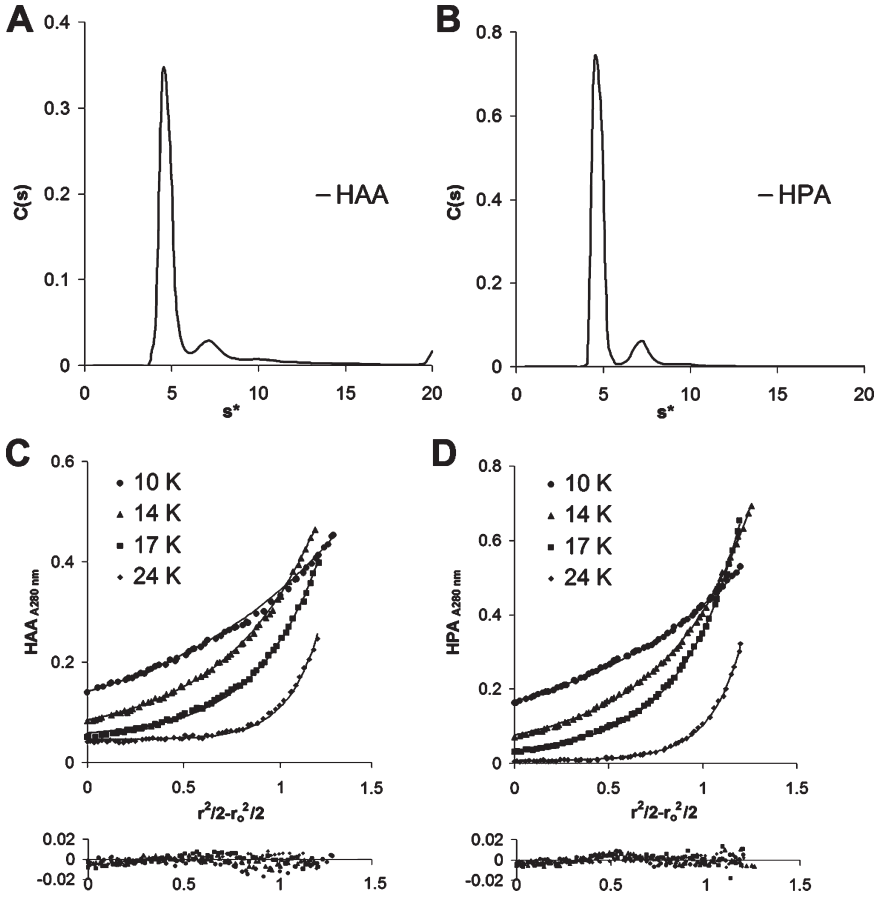

FIGURE 3: Analytical ultracentrifugation analysis of lectins HAA and HPA. Sedimentation velocity analysis of (A) HAA and (B) HPA. Each lectin at 3.7 μM was spun at 36000 rpm in a Beckman XL-I analytical ultracentrifuge. Data were fitted using the $c(s)$ sedimentation analysis routines in SEDFIT to yield the differential sedimentation coefficient distribution for each sample. HAA and HPA sedimented with sedimentation coefficients of 4.8 and 4.7 S and apparent molecular masses of ~86.8 and ~77.9 kDa, respectively. On the basis of the amino acid sequence of HPA and expected levels of *N*-glycosylation, the sedimentation data suggest that these lectins sediment mainly as a hexamer. A relatively small amount of dodecamer (~150−171 kDa) was also present in each sample. Sedimentation equilibrium analysis of (C) HAA and (D) HPA at concentrations ranging from 0.353 to 2 μM at rotor speeds of 10000, 14000, 17000, and 24000 rpm. Using WinNONLIN, data were globally fitted to determine σ_w, the weight-average buoyant molecular mass. The experimental molecular mass based on σ_w was calculated to be 81102 Da (76240−85950 Da) for HAA and 86690 Da (82708−90671 Da) for HPA, confirming that these lectins form hexamers.

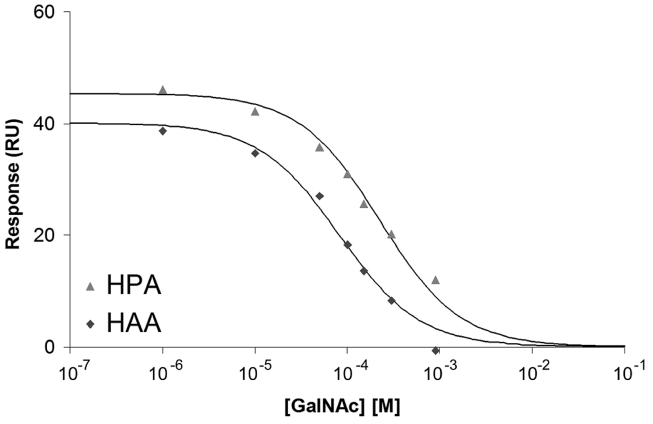

FIGURE 4: Competition biosensor assay of HAA and HPA binding to GalNAc. HAA and HPA were immobilized on the sensor chip, and 8 μM mIgA1κ was co-injected with varying concentrations of GalNAc. The IC_{50} for GalNAc binding to the lectins was determined using Scientist.

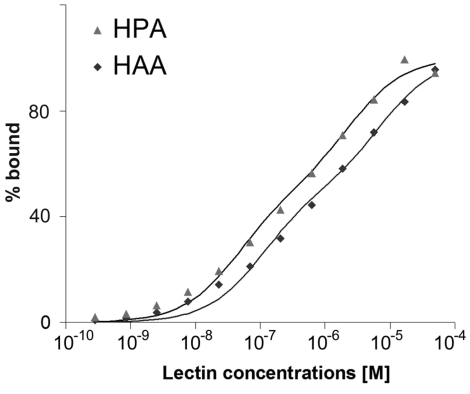

FIGURE 5: Equilibrium binding isotherms for HAA and HPA binding to the HR-GalNAc glycopeptide. HR-GalNAc was immobilized on the sensor chip, and HAA or HPA was injected over the chip. Data points were determined by averaging the equilibrium response at the plateau of each binding curve and fitted to a two-site model in Scientist.

(in molar equivalents) on the chip was high relative to the density of the IgA1 samples described below. This high density would favor multivalent interactions of GalNAc on the hinge glycopeptide with the hexameric lectins. In general, lectins are often multimeric, with low single-site affinities for individual carbohydrate residues but much higher apparent affinities for surfaces containing multiple carbohydrate receptors (*59*).

SPR Analysis of Lectin Binding to IgA1 Myeloma Proteins. Techniques such as ELISA and lectin blots have been

used to study aberrantly glycosylated IgA1 myeloma proteins (*48*). Although these techniques yield higher-intensity signals for Gal-deficient IgA1 than for control IgA1, we wanted to determine whether the apparently higher degree of binding by the lectin was due to a higher affinity for Gal-deficient IgA1 or to a higher stoichiometry of binding, i.e., a larger number of lectins bound per IgA1 molecule. It was also of interest to assess whether HAA and HPA could accurately detect undergalactosylated IgA1 hinge-region glycans in the absence of neuraminidase treatment to remove the sialic acid residues. We analyzed the binding of HAA and HPA to several Gal-deficient IgA1 samples from myeloma patients using SPR. $IgA1_{Ale}$ exhibited the strongest binding by both HAA and HPA, while $IgA1_{Mce}$ had the lowest affinity (Figure 6). The affinities of each IgA1 myeloma protein for HAA and HPA are listed in Tables 2 and 3. The $IgA1_{Ale}$ SPR results are consistent with the lectin blots that showed that this sample had the strongest signal. However, there were some discrepancies between the SPR and lectin data with regard to other samples. In particular, the lectin blots showed a stronger signal for $IgA1_{Mce}$ than for IgA1κ and IgA1λ. In the SPR assay, irrespective of the molecular form of IgA1 [i.e., monomeric (m) or polymeric (p)], the binding to both lectins followed a trend: $IgA1_{Ale}$ > IgA1κ > IgA1λ > $IgA1_{Mce}$. Furthermore, the same trend ($IgA1_{Ale}$ > IgA1κ > IgA1λ) and overall similar apparent affinities were obtained if the orientation was reversed such that the lectins were immobilized on the chip and the IgA1 samples flowed over the chip (Figure 7 and Table 4).

Biosensor-Based Analysis of Lectin Binding to IgA1 Derived from EBV-Immortalized IgA1-Secreting Cell Lines from Patients. Moore et al. (*48*) used a capture ELISA to show that HAA distinguished serum IgA1 of IgAN patients from that of healthy controls, with a high level of statistical significance (p = 0.0003). An improved quantitative lectin ELISA confirmed that galactosylation of *O*-glycans in the IgA1 hinge region differed between IgAN patients and healthy controls, and the assay differentiated the two groups of individuals with high sensitivity and specificity (*3*). To further analyze the ability of HAA or HPA to discriminate between aberrantly glycosylated and normally glycosylated IgA1 hinge-region glycans, we conducted equilibrium biosensor analyses using IgA1 purified from the supernatants of EBV-immortalized IgA1-secreting cell lines from IgAN patients and healthy controls (*9*)

Table 1: Equilibrium Parameters for HAA and HPA Lectins Binding to HR-GalNAc at 25 °C[a]

analyte	K_D1 (μM)	K_D2 (μM)
HPA	0.045 ± 0.006	2.3 ± 0.6
HAA	0.11 ± 0.01	7 ± 2

[a] K_D values were derived using a two-site model in Scientist. Equilibrium binding parameters for HR-GalNAc were derived from global analyses of two independent experiments each with 12 different concentrations of injected analyte (HAA or HPA).

Table 2: Equilibrium Parameters for HAA Binding to IgA1 Myeloma Proteins at 25 °C[a]

ligand	K_D1 (μM)	K_D2 (μM)
$mIgA1_{Ale}$	0.6 ± 0.1	21 ± 17
$pIgA1_{Ale}$	1.0 ± 0.3	14 ± 5
mIgA1κ	1.8 ± 0.6	8 ± 3
pIgA1κ	1.7 ± 0.1	25 ± 9
mIgA1λ	6.2 ± 0.6	73 ± 9
pIgA1λ	3.0 ± 0.6	28 ± 8
$mIgA1_{Mce}$	7.2 ± 0.7	76 ± 9
$pIgA1_{Mce}$	5.6 ± 0.2	70 ± 4

[a] K_D values were derived using a two-site model in Scientist. Equilibrium binding parameters for the different IgA1 myeloma proteins were derived from analyses with 11 different concentrations of injected HAA.

Table 3: Equilibrium Parameters for HPA Binding to IgA1 Myeloma Proteins at 25 °C[a]

ligand	K_D1 (μM)	K_D2 (μM)
$mIgA1_{Ale}$	0.29 ± 0.04	10 ± 4
$pIgA1_{Ale}$	0.58 ± 0.10	6 ± 2
mIgA1κ	0.76 ± 0.07	10 ± 2
pIgA1κ	0.65 ± 0.08	11 ± 4
mIgA1λ	1.8 ± 0.2	21 ± 3
pIgA1λ	1.1 ± 0.4	5 ± 1
$mIgA1_{Mce}$	2.3 ± 0.3	24 ± 13
$pIgA1_{Mce}$	1.1 ± 0.4	7 ± 5

[a] K_D values were derived using a two-site model in Scientist. Equilibrium binding parameters for the different IgA1 myeloma proteins were derived from analyses with 11 different concentrations of injected HPA.

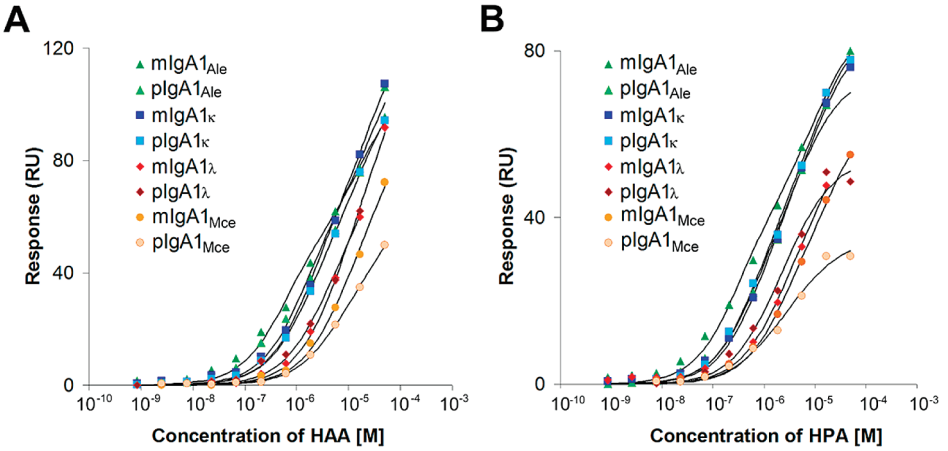

FIGURE 6: Equilibrium binding isotherms for HAA and HPA binding to different IgA1 myeloma proteins. Equilibrium binding experiments were performed by immobilization of (A) HAA and (B) HPA on a biosensor chip and injection of various IgA1 myeloma proteins over the chip. Data points were determined by averaging the equilibrium response at the plateau of each binding curve and fitted to a two-site model in Scientist. The order of the affinities for the IgA1 myeloma proteins binding to HAA and HPA was as follows: $IgA1_{Ale}$ > IgA1κ > IgA1λ > $IgA1_{Mce}$.

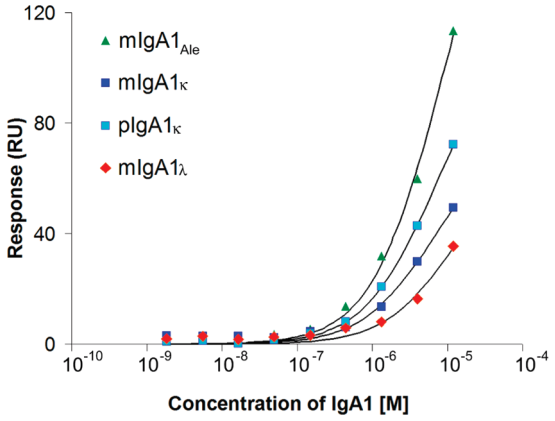

FIGURE 7: Equilibrium binding isotherms for different IgA1 myeloma proteins binding to the HAA ligand. Equilibrium binding experiments were performed by immobilization of HAA on a biosensor chip and injection of various IgA1 myeloma proteins. Data points representing steady-state responses were fitted to a two-site model. The order of the binding affinities of the different IgA1 myeloma proteins for HAA was as follows, irrespective of the orientation in which the experiment was performed: $IgA1_{Ale}$ > IgA1κ > IgA1λ.

Table 4: Equilibrium Parameters for IgA1 Myeloma Proteins Binding to the HAA Ligand at 25 °C[a]

analyte	K_D1 (μM)	K_D2 (μM)
$mIgA1_{Ale}$	2.1 ± 0.2	12 ± 2
mIgA1κ	3.7 ± 0.7	23 ± 6
pIgA1κ	3.9 ± 0.2	27 ± 3
mIgA1λ	7 ± 3	41 ± 21

[a] K_D values were derived using a two-site model in Scientist. Equilibrium binding parameters for HAA were derived from analyses with nine different concentrations of injected IgA1.

(Figure 8). Both lectins recognized the Gal-deficient IgA1 from IgAN patients with high apparent affinity but had a much lower affinity for the IgA1 from healthy controls (Tables 5 and 6). Indeed, we were unable to fit the binding curve from one of the healthy controls because of the extremely weak response. The apparent affinities of HAA and HPA for the IgA1 in the samples from IgAN patients were comparable to those for $IgA1_{Ale}$ but were still weaker than those for the idealized HR-GalNAc glycopeptide. In contrast, the IgA1 in the samples from healthy controls showed much weaker apparent affinities than those observed for any of the IgA1 myeloma proteins. To compare the degree of sialylation of IgA1 samples, we used the lectins SNA and MAA-II to assay for α-2,6-linked and α-2,3-linked sialic acid moieties, respectively. SNA exhibited similar apparent affinities for each patient-derived IgA1 sample (Figure 8C), indicating similar levels of α-2,6-linked sialic acid attached to their *N*- and *O*-glycans. MAA-II binding indicated greater variability in the levels of α-2,3-linked sialic acid; in particular, the IgA1 sample from IgAN patient 1 exhibited a very low apparent affinity for MAA-II, suggesting very low levels of α-2,3-linked sialic acid (Figure 8D).

DISCUSSION

As the clinical diagnosis of IgAN currently requires a kidney biopsy, the development of reliable serum-based testing is of great importance. Moore et al. (*48*) and Moldoveanu et al. (*3*) have shown that HAA can be used for detection of Gal-deficient IgA1 in IgAN patients. This study was conducted to improve our understanding of the mechanism by which HAA and HPA lectins recognize the Gal-deficient IgA1 hinge region. Although other lectins such as *Wisteria floribunda* lectin (WFA), *Vicia villosa* agglutinin (VVA), and soybean agglutinin (SBA) are considered to be GalNAc-binding lectins, Tachibana et al. (*60*) demonstrated that these in fact did not bind to GalNAc-conjugated peptides and thus were not analyzed here.

Various methods, such as mass spectrometry, monosaccharide composition analysis, lectin-based ELISA, and Western blotting, have been used to assess Gal deficiency in the *O*-glycans of serum IgA1 as well as IgA1 in the glomeruli of IgAN patients (*2*, *3*, *5*−*9*, *28*, *30*, *48*, *50*, *57*, *58*, *61*−*63*). Mass spectrometry is extremely informative but not commonly used for high-throughput diagnostic analyses. HAA- and HPA-based ELISAs and Western blotting have been useful in analyses of IgA1 from IgAN patients (*2*, *3*, *6*−*9*, *28*, *30*, *48*, *50*); however, depending on the lectin source, variability in binding characteristics and assay-dependent differences in binding were observed with various IgA1 myeloma proteins (*48*). To analyze lectin binding in more detail, we have used a sensor chip-based real-time binding assay to systematically analyze how these lectins recognize Gal-deficient IgA1. Our data showed that HAA and HPA bound to the HR-GalNAc glycopeptide that resembles the antigenic epitope(s) in IgAN patients, with nanomolar to low micromolar apparent affinity (Figure 5 and Table 1). This apparent affinity is much higher than the reported single-site affinity of 130 μM for HPA binding to GalNAc (*51*); this apparent difference is clearly due to an avidity effect due to multivalent interactions of the lectins with HR-GalNAc coupled at relatively high density to the chip surface. Both lectins bound to all four IgA1 myeloma proteins, with the highest apparent affinity for $IgA1_{Ale}$ in the lectin blots and biosensor experiments (Figures 2, 6, and 7 and Tables 2−4). The higher apparent affinity for $IgA1_{Ale}$ is presumably due to an increased number of exposed GalNAc residues available for these lectins to bind.

In all the samples tested by SPR, HAA and HPA exhibited the same trends in binding to an identical panel of ligands, although HPA reproducibly bound with slightly higher apparent affinities. However, we observed discrepancies between the trends shown with SPR and lectin blots. In lectin blots, the binding trend for HAA and HPA was as follows: $IgA1_{Ale}$ > IgA1κ > $IgA1_{Mce}$ > IgA1λ. In the biosensor assay, the binding trend was as follows: $IgA1_{Ale}$ > IgA1κ > IgA1λ > $IgA1_{Mce}$. This discrepancy is likely due to differences in the way the IgA1 glycans are presented in the different experiments. In SPR, the IgA1 samples are maintained in their native folded state, whereas for lectin blotting, IgA1 was reduced and denatured during SDS−PAGE separation before being transferred onto the membrane. It is possible that binding of HAA or HPA to one or more exposed GalNAc residues in $IgA1_{Mce}$ is sterically hindered in the native state. For example, FT-ICR mass spectrometry studies by Renfrow et al. (*24*, *26*) mapped the site-specific *O*-glycoforms of $IgA1_{Mce}$, showing five major glycopeptide species that contained four to six *O*-glycan sites. Of the most abundant variant glycopeptides, two were fully galactosylated (glycopeptides with four GalNAc and four Gal residues or five GalNAc and five Gal residues), and two others had a single exposed GalNAc residue, located at S232 (in the glycopeptide with four GalNAc and three Gal residues) or at either T233 or T236 (in the glycopeptide with five GalNAc and four Gal residues). The low-resolution structure of IgA1, determined by small-angle X-ray and neutron scattering, revealed that

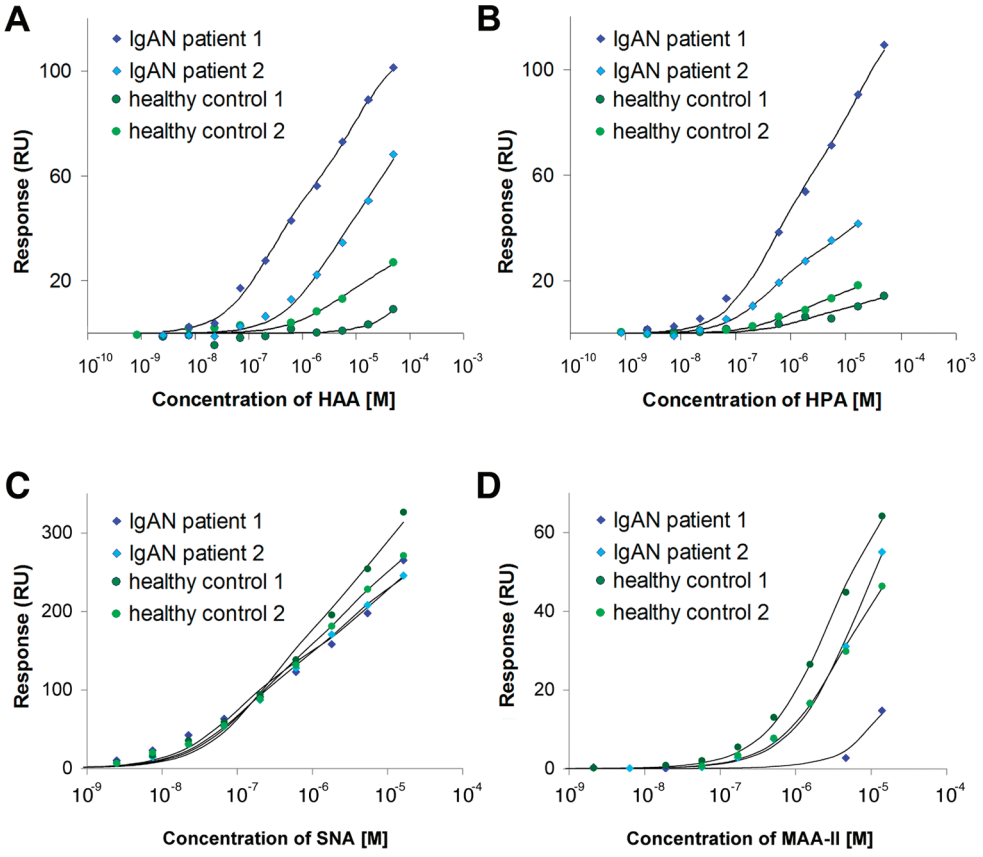

FIGURE 8: Equilibrium binding isotherms for HAA and HPA binding to IgA1 derived from IgAN patients and healthy controls. Equilibrium binding experiments were performed by immobilization of IgA1 proteins secreted by IgA1-producing cells from healthy controls and IgAN patients on a sensor chip and injection of (A) HAA, (B) HPA, (C) SNA, or (D) MAA-II over the chip. Data points representing steady-state responses were fitted to a two-site model. HAA and HPA bind to IgA1 secreted by IgA1-secreting cells of IgAN patients with a much higher affinity than to IgA1 from healthy controls, suggesting that these lectins could be used as diagnostic reagents to detect the disease-specific glycosylation aberrancy. SNA bound similarly to all IgA1 samples, indicating similar levels of α-2,6-linked sialic acid. MAA-II bound to IgA1 from IgAN patient 1 much more weakly than to the other IgA1 samples, indicating lower levels of α-2,3-linked sialic acid.

Table 5: Equilibrium Parameters for HAA Lectin Binding at 25 °C to IgA1 Proteins Secreted by IgA1-Producing Cells[a]

ligand IgA1 source	K_D1 (μM)	K_D2 (μM)
IgAN patient 1	0.6 ± 0.2	26 ± 3
IgAN patient 2	1.2 ± 0.2	31 ± 5
healthy control 1	–	–
healthy control 2	20 ± 6	270 ± 200

[a] K_D values were derived using a two-site model in Scientist. Equilibrium parameters for IgA1 proteins secreted by IgA1-producing cells were derived from analyses with 11 different concentrations of injected HAA. The dashes for healthy control 1 indicate that the binding to HAA was weak and the affinities could not be determined at the concentrations of analyte (HAA) used in the experiment.

Table 6: Equilibrium Parameters for HPA Lectin Binding at 25 °C to IgA1 Proteins Secreted by IgA1-Producing Cells[a]

ligand IgA1 source	K_D1 (μM)	K_D2 (μM)
IgAN patient 1	0.61 ± 0.05	23 ± 2
IgAN patient 2	1.0 ± 0.7	17 ± 6
healthy control 1	–	–
healthy control 2	22 ± 7	130 ± 80

[a] K_D values were derived using a two-site model in Scientist. Equilibrium parameters for IgA1 proteins secreted by IgA1-producing cells were derived from analyses with 11 different concentrations of injected HPA. The dashes for healthy control 1 indicate that the binding to HPA was weak and the affinities could not be determined at the concentrations of analyte (HPA) used in the experiment.

IgA1 adopts a T-shaped conformation, with the C-terminal portion of the hinge in the proximity of the Fc region (*64*). Depending on the precise orientation of the Ser or Thr side chains and rotation about the glycosidic bond, it is possible that an exposed GalNAc at one of these positions (S232, T233, or T236) of IgA1 in the native state would be inaccessible to the lectins, particularly in the case of T233 or T236. Moore et al. also found that HPA was able to recognize a particular IgA1 myeloma protein (Kni) when denatured in a lectin blot but not in its native form by an ELISA (*48*). Furthermore, Moore et al. reported systematic differences between the results from lectin blots and those from the ELISA and suggested that the specific three-dimensional configuration of the hinge region played an important role in lectin recognition (*48*). These discrepancies between the lectin blot and either SPR or ELISA may have functional significance, given that GalNAc residues that are inaccessible to HAA or HPA would likely also be inaccessible to anti-glycan antibodies in the circulation of IgAN patients. Thus, a diagnostic assay that relies on denatured IgA1 (such as a lectin blot) might overestimate the pathogenicity of a particular Gal-deficient IgA1 sample compared to an assay (like SPR or ELISA) that utilizes native IgA1 samples.

In this study, we have used a biophysical approach to analyze the interaction of HAA and HPA with homogeneous samples of

IgA1 purified from culture media from EBV-immortalized IgA1-secreting cells from IgAN patients and healthy controls. The lectin blotting and SPR assays showed that HAA and HPA bound much more tightly to IgA1 originating from IgAN patients than to IgA1 from healthy controls (Figures 2 and 8 and Tables 5 and 6). Furthermore, we have compared the apparent lectin affinities for IgA1 from patients with IgAN and from healthy controls with the affinities of the myeloma proteins and HR-GalNAc glycopeptide. The apparent lectin affinities for the IgA1 secreted by the cells of patients were greater than those for $IgA1_{Mce}$, comparable to those for $IgA1_{Ale}$, but weaker than those for the HR-GalNAc glycopeptide. Another interesting feature of the binding curves for patient 2 and both healthy controls is the fact that the maximal response appeared to be significantly weaker than for patient 1 or the IgA1 myeloma proteins, despite coupling comparable levels of IgA1 proteins to the chip. This finding may indicate heterogeneity in the *O*-glycosylation pattern of the hinge region; i.e., only a fraction of the total population of the IgA1 samples contained Gal-deficient hinge-region glycans, or those hinge regions have relatively few exposed (terminal) GalNAc residues. When normalized to the same maximum, both patient samples exhibited similar apparent affinities for HAA and HPA, although IgA1 from patient 2 still bound more weakly. In terms of the IgA1 myeloma proteins, $IgA1_{Mce}$ contains a single exposed GalNAc in approximately 60% of the sample (*24*, *26*), whereas $IgA1_{Ale}$ contains a single exposed GalNAc in 46% of the sample and two exposed GalNAc residues in 12% of the sample (K. Takahashi, J. Novak, and M. B. Renfrow, personal communication). However, $IgA1_{Mce}$ is extensively sialylated, while $IgA1_{Ale}$ contains very little sialic acid. In contrast, the synthetic HR-GalNAc glycopeptide is a homogeneous sample that contains three exposed GalNAc residues. Thus, we predict that more than half of the *O*-glycans on IgA1 from patient 1 are Gal-deficient, with average levels of GalNAc exposure approximately equal to that of $IgA1_{Ale}$ (with one or two GalNAc residues per hinge). In contrast, a lower percentage of the IgA1 from patient 2 appears to contain Gal-deficient IgA1 hinge region glycans, although the degree of GalNAc exposure within this subpopulation is comparable to that for IgA1 from patient 1.

Some of the observed differences between the two IgAN patient-derived samples could be attributed to differential sialylation, as we have previously shown that ~50% of Gal-deficient *O*-glycans on IgA1 from patients with IgAN are sialylated (*9*). We now analyzed this directly using two sialic acid-specific lectins: SNA (specific for α-2,6-linked sialic acid on both *N*- and *O*-glycans of IgA1) (Table 7) and MAA-II (specific for α-2,3-linked sialic acid, predominantly on *O*-glycans) (Table 8). We found that both IgAN patient-derived IgA1 and healthy control-derived IgA1 exhibited similar affinities for SNA (Figure 8C), suggesting that the IgA1 proteins have similar levels of α-2,6-linked sialic acid. This result pertains to both the *O*-glycans (*9*) and the *N*-glycans; it has previously been demonstrated that 90−100% of sialylated *N*-glycans on IgA1 have the α-2,6 linkage (*13*, *22*, *27*). In contrast, IgA1 from IgAN patient 1 had a much lower affinity for MAA-II than IgA1 from IgAN patient 2 or the healthy controls (Figure 8D). In IgA1, α-2,3-linked sialic acids are typically attached to the terminal Gal residue on *O*-glycans (Figure 1) and only rarely are found on *N*-glycans (*13*, *22*, *27*). Thus, the MAA-II data are consistent with the HAA and HPA data and indicate that IgA1 from IgAN patient 1 has a higher proportion of exposed GalNAc residues compared to IgA1 in the other samples.

Table 7: Equilibrium Parameters for SNA Lectin Binding at 25 °C to IgA1 Proteins Secreted by IgA1-Producing Cells[a]

ligand IgA1 source	K_D1 (μM)	K_D2 (μM)
IgAN patient 1	0.10 ± 0.05	~7
IgAN patient 2	0.12 ± 0.01	4 ± 2
healthy control 1	0.22 ± 0.07	~8
healthy control 2	0.15 ± 0.02	5 ± 3

[a] K_D values were derived using a two-site model in Scientist. Equilibrium parameters for IgA1 proteins secreted by IgA1-producing cells were derived from analyses with 10 different concentrations of injected SNA. K_D2 values for IgAN patient 1 and healthy control 1 could not be determined with a high degree of confidence under the conditions that were used.

Table 8: Equilibrium Parameters for MAA-II Lectin Binding at 25 °C to IgA1 Proteins Secreted by IgA1-Producing Cells[a]

ligand IgA1 source	K_D (μM)
IgAN patient 1	–
IgAN patient 2	6.8 ± 0.8
healthy control 1	3.0 ± 0.2
healthy control 2	4.3 ± 0.4

[a] K_D values were derived using a one-site model in Scientist. Equilibrium parameters for IgA1 proteins secreted by IgA1-producing cells were derived from analyses with 10 different concentrations of injected MAA-II. The dash for IgAN patient 1 indicates that the binding to MAA-II was weak and the affinities could not be determined at the concentrations of analyte (MAA-II) used in the experiment.

The sedimentation data presented here indicate that HAA and HPA adopt nearly identical shapes and assembly states in solution: predominantly hexamers, with low levels of dodecamers. Furthermore, competition binding studies with GalNAc and direct binding analyses with HR-GalNAc and a panel of IgA1 samples revealed very similar behavior between these two lectins. These data allow us to propose a general model for the recognition of Gal-deficient IgA1 hinge-region glycans by these lectins. The crystal structure of HPA showed that it exists as a hexamer, consistent with our AUC results (*51*). Each protomer of HPA adopts a β-barrel fold and assembles into a noncovalent trimer. Two HPA trimers are linked back to back by disulfide bridges to form the hexamer that is the biologically relevant species. Preliminary X-ray structural analysis of HAA indicates that it forms a hexamer with the same back-to-back arrangement of noncovalent trimers observed for HPA (M. M. Gomes and A. B. Herr, unpublished data). The GalNAc-binding sites are located at the distal end of each HPA trimer, approximately 20 Å apart (*51*). The distance between binding sites on opposite trimers is 75−80 Å [i.e., along the long axis of the elongated hexamer (Figure 9)]. On the basis of the location of the binding sites on the exterior of the HPA trimer and the inherent 3-fold rotational symmetry between these sites, it appears that each HPA trimer (i.e., one end of the hexamer) could bind only one GalNAc residue at a time in a given IgA1 hinge region. Thus, we propose that HPA and HAA act as functionally bivalent lectins when binding to IgA1, with each trimeric end of the HPA or HAA hexamer binding to a single GalNAc residue. Our data strongly support this conclusion, given that the apparent affinities of the lectins for IgA1 samples are similar regardless of which protein is coupled to the chip and which is injected (Figures 6 and 7 and Tables 2 and 4). In contrast, a case in which one binding partner has a higher valency than the other will show a significant difference in apparent affinity when the orientation is reversed.

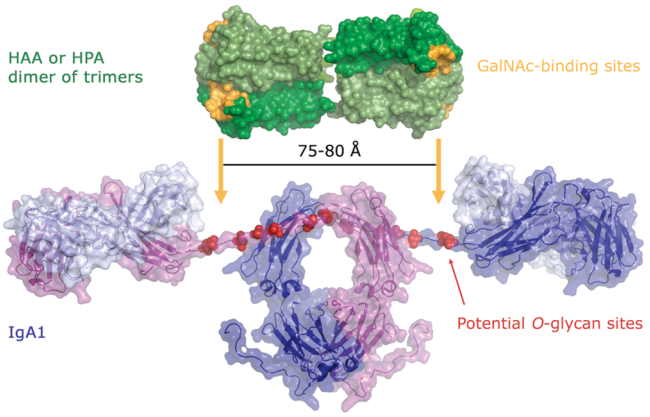

FIGURE 9: Model for bivalent binding of HAA or HPA to a single molecule of undergalactosylated monomeric IgA1. The HAA and HPA lectins form hexamers made up of dimers of trimers (various green shades according to subunit). The GalNAc-binding sites are located at the outer extremities (yellow) and are separated by ~75−80 Å along the long axis of the hexamer (*51*). Each face of the HAA−HPA hexamer exposes two binding sites that could interact simultaneously with GalNAc residues on the two hinges of IgA1. IgA1 heavy and light chains are shown in different shades of blue and purple, respectively, with the Ser and Thr residues that are potentially *O*-glycosylated shown as red spheres. Note that this model of IgA1 is one possible conformation (*64*), but the hinge region with the *O*-glycans is expected to be flexible, resulting in multiple conformational states of IgA1 that could be recognized by HAA or HPA, given the similarity in spacing between the GalNAc-binding sites on the HAA−HPA hexamer and the location of potentially undergalactosylated *O*-glycans on the IgA1 hinges.

For example, binding of FcαRI (a monovalent receptor) to the Fc region of IgA1 (a bivalent ligand) shows an apparent affinity of 9 nM when IgA1-Fc is injected and FcαRI is coupled, compared to affinities of 200−400 nM when FcαRI is injected over IgA1-Fc (*55*). In the case of HPA and HAA (functionally bivalent) binding to IgA1 (bivalent), the same binding trends and similar apparent affinities are observed in either orientation, suggesting that the valencies of the lectin and IgA1 are equivalent. According to the solution scattering structure of intact IgA1, the maximal distance between the potential *O*-glycosylation sites on the two hinge regions in a single mIgA1 molecule is approximately 88 Å, comparable to the separation between binding sites on opposite ends of the HPA hexamer (Figure 9) (*64*). Thus, the functionally bivalent lectin could potentially bridge both hinge regions in a single IgA1 molecule or bind to hinge regions of two different IgA1 molecules when they are coupled to a surface.

The functionally bivalent nature of HAA and HPA binding to the IgA1 hinge has implications for the development of diagnostic tools for IgAN. The bivalent interaction increases the apparent affinity of binding dramatically when compared to the affinity of HAA or HPA for a single GalNAc residue; this phenomenon will reduce the level of nonspecific binding to alternate targets. Injecting patient serum (or serum-purified IgA) over a sensor chip coated with HAA or HPA (possibly complemented with MAA-II) could be used to rapidly screen patients to identify those with severely Gal-deficient IgA1. This approach has the potential to be faster, safer, and cheaper than the kidney biopsy analysis that is the current standard for diagnosis of IgAN. Furthermore, in contrast to the previous methods used to study *O*-glycans in the IgA1 hinge region, a biosensor-based assay provides a rapid, quantitative, highly sensitive method requiring small quantities of sample that is independent of experimental orientation. In addition, in our SPR assay, the monomeric and polymeric forms of IgA1 in the samples exhibited similar affinities for HAA and HPA (Figure 6). This point is important because serum Gal-deficient IgA1 is predominantly polymeric. The results presented here indicate that a biosensor-based assay could be developed into a rapid, point-of-care diagnostic device. It will be interesting in future studies to determine if there is a particular threshold of exposed GalNAc residues on the IgA1 hinge region that leads to the development of IgAN symptoms or to end-stage renal failure.

ACKNOWLEDGMENT

We thank Catherine V. Barker for assistance with collection of blood samples and Rhubell Brown and Stacy Hall for technical assistance with protein purification.

SUPPORTING INFORMATION AVAILABLE

Information about one-site versus two-site fits of the binding data as well as representative raw sensorgram data from the SPR experiments. This material is available free of charge via the Internet at http://pubs.acs.org.

REFERENCES

1. Basset, C., Durand, V., Jamin, C., Clement, J., Pennec, Y., Youinou, P., Dueymes, M., and Roitt, I. M. (2000) Increased *N*-linked glycosylation leading to oversialylation of monomeric immunoglobulin A1 from patients with Sjögren's syndrome. *Scand. J. Immunol. 51*, 300–306.
2. Lau, K. K., Wyatt, R. J., Moldoveanu, Z., Tomana, M., Julian, B. A., Hogg, R. J., Lee, J. Y., Huang, W. Q., Mestecky, J., and Novak, J. (2007) Serum levels of galactose-deficient IgA in children with IgA nephropathy and Henoch-Schönlein purpura. *Pediatr. Nephrol. 22*, 2067–2072.
3. Moldoveanu, Z., Wyatt, R. J., Lee, J. Y., Tomana, M., Julian, B. A., Mestecky, J., Huang, W. Q., Anreddy, S. R., Hall, S., Hastings, M. C., Lau, K. K., Cook, W. J., and Novak, J. (2007) Patients with IgA nephropathy have increased serum galactose-deficient IgA1 levels. *Kidney Int. 71*, 1148–1154.
4. Saulsbury, F. T. (1997) Alterations in the *O*-linked glycosylation of IgA1 in children with Henoch-Schönlein purpura. *J. Rheumatol. 24*, 2246–2249.
5. Mestecky, J., Tomana, M., Crowley-Nowick, P. A., Moldoveanu, Z., Julian, B. A., and Jackson, S. (1993) Defective galactosylation and clearance of IgA1 molecules as a possible etiopathogenic factor in IgA nephropathy. *Contrib. Nephrol. 104*, 172–182.
6. Allen, A. C., Harper, S. J., and Feehally, J. (1995) Galactosylation of *N*- and *O*-linked carbohydrate moieties of IgA1 and IgG in IgA nephropathy. *Clin. Exp. Immunol. 100*, 470–474.
7. Tomana, M., Matousovic, K., Julian, B. A., Radl, J., Konecny, K., and Mestecky, J. (1997) Galactose-deficient IgA1 in sera of IgA nephropathy patients is present in complexes with IgG. *Kidney Int. 52*, 509–516.
8. Tomana, M., Novak, J., Julian, B. A., Matousovic, K., Konecny, K., and Mestecky, J. (1999) Circulating immune complexes in IgA nephropathy consist of IgA1 with galactose-deficient hinge region and antiglycan antibodies. *J. Clin. Invest. 104*, 73–81.
9. Suzuki, H., Moldoveanu, Z., Hall, S., Brown, R., Vu, H. L., Novak, L., Julian, B. A., Tomana, M., Wyatt, R. J., Edberg, J. C., Alarcon, G. S., Kimberly, R. P., Tomino, Y., Mestecky, J., and Novak, J. (2008) IgA1-secreting cell lines from patients with IgA nephropathy produce aberrantly glycosylated IgA1. *J. Clin. Invest. 118*, 629–639.
10. Zickerman, A. M., Allen, A. C., Talwar, V., Olczak, S. A., Brownlee, A., Holland, M., Furness, P. N., Brunskill, N. J., and Feehally, J. (2000) IgA myeloma presenting as Henoch-Schönlein purpura with nephritis. *Am. J. Kidney Dis. 36*, E19.
11. Allen, A. C., Willis, F. R., Beattie, T. J., and Feehally, J. (1998) Abnormal IgA glycosylation in Henoch-Schönlein purpura restricted to patients with clinical nephritis. *Nephrol., Dial., Transplant. 13*, 930–934.
12. Lasseur, C., Allen, A. C., Deminiere, C., Aparicio, M., Feehally, J., and Combe, C. (1997) Henoch-Schönlein purpura with immunoglobulin A nephropathy and abnormalities of immunoglobulin A in a Wiskott-Aldrich syndrome carrier. *Am. J. Kidney Dis. 29*, 285–287.

13. Baenziger, J., and Kornfeld, S. (1974) Structure of the carbohydrate units of IgA1 immunoglobulin. I. Composition, glycopeptide isolation, and structure of the asparagine-linked oligosaccharide units. *J. Biol. Chem. 249*, 7260–7269.
14. Baenziger, J., and Kornfeld, S. (1974) Structure of the carbohydrate units of IgA1 immunoglobulin. II. Structure of the *O*-glycosidically linked oligosaccharide units. *J. Biol. Chem. 249*, 7270–7281.
15. Tomana, M., Niedermeier, W., Mestecky, J., and Skvaril, F. (1976) The differences in carbohydrate composition between the subclasses of IgA immunoglobulins. *Immunochemistry 13*, 325–328.
16. Torano, A., Tsuzukida, Y., Liu, Y. S., and Putnam, F. W. (1977) Location and structural significance of the oligosaccharides in human Ig-A1 and IgA2 immunoglobulins. *Proc. Natl. Acad. Sci. U.S.A. 74*, 2301–2305.
17. Liu, Y.-S. V., Low, T. L. K., Infante, A., and Putnam, F. W. (1976) Complete covalent structure of a human IgA1 immunoglobulin. *Science 193*, 1017–1019.
18. Gomes, M. M., Wall, S. B., Takahashi, K., Novak, J., Renfrow, M. B., and Herr, A. B. (2008) Analysis of IgA1 *N*-glycosylation and its contribution to FcαRI binding. *Biochemistry 47*, 11285–11299.
19. Frangione, B., and Wolfenstein-Todel, C. (1972) Partial duplication in the "hinge" region of IgA 1 myeloma proteins. *Proc. Natl. Acad. Sci. U.S.A. 69*, 3673–3676.
20. Field, M. C., Dwek, R. A., Edge, C. J., and Rademacher, T. W. (1989) *O*-linked oligosaccharides from human serum immunoglobulin A1. *Biochem. Soc. Trans. 17*, 1034–1035.
21. Iwase, H., Tanaka, A., Hiki, Y., Kokubo, T., Ishii-Karakasa, I., Kobayashi, Y., and Hotta, K. (1996) Estimation of the number of *O*-linked oligosaccharides per heavy chain of human serum IgA1 by matrix-assisted laser desorption ionization time-of-flight mass spectrometry (MALDI-TOFMS) analysis of the hinge glycopeptide. *J. Biochem. 120*, 393–397.
22. Mattu, T. S., Pleass, R. J., Willis, A. C., Kilian, M., Wormald, M. R., Lellouch, A. C., Rudd, P. M., Woof, J. M., and Dwek, R. A. (1998) The glycosylation and structure of human serum IgA1, Fab, and Fc regions and the role of *N*-glycosylation on Fcα receptor interactions. *J. Biol. Chem. 273*, 2260–2272.
23. Novak, J., Tomana, M., Kilian, M., Coward, L., Kulhavy, R., Barnes, S., and Mestecky, J. (2000) Heterogeneity of *O*-glycosylation in the hinge region of human IgA1. *Mol. Immunol. 37*, 1047–1056.
24. Renfrow, M. B., Cooper, H. J., Tomana, M., Kulhavy, R., Hiki, Y., Toma, K., Emmett, M. R., Mestecky, J., Marshall, A. G., and Novak, J. (2005) Determination of aberrant *O*-glycosylation in the IgA1 hinge region by electron capture dissociation Fourier transform-ion cyclotron resonance mass spectrometry. *J. Biol. Chem. 280*, 19136–19145.
25. Tarelli, E., Smith, A. C., Hendry, B. M., Challacombe, S. J., and Pouria, S. (2004) Human serum IgA1 is substituted with up to six *O*-glycans as shown by matrix assisted laser desorption ionisation time-of-flight mass spectrometry. *Carbohydr. Res. 339*, 2329–2335.
26. Renfrow, M. B., Mackay, C. L., Chalmers, M. J., Julian, B. A., Mestecky, J., Kilian, M., Poulsen, K., Emmett, M. R., Marshall, A. G., and Novak, J. (2007) Analysis of *O*-glycan heterogeneity in IgA1 myeloma proteins by Fourier transform ion cyclotron resonance mass spectrometry: Implications for IgA nephropathy. *Anal. Bioanal. Chem. 389*, 1397–1407.
27. Field, M. C., Amatayakul-Chantler, S., Rademacher, T. W., Rudd, P. M., and Dwek, R. A. (1994) Structural analysis of the *N*-glycans from human immunoglobulin A1: Comparison of normal human serum immunoglobulin A1 with that isolated from patients with rheumatoid arthritis. *Biochem. J. 299* (Part 1), 261–275.
28. Allen, A. C., Bailey, E. M., Brenchley, P. E., Buck, K. S., Barratt, J., and Feehally, J. (2001) Mesangial IgA1 in IgA nephropathy exhibits aberrant *O*-glycosylation: Observations in three patients. *Kidney Int. 60*, 969–973.
29. Hiki, Y., Horii, A., Iwase, H., Tanaka, A., Toda, Y., Hotta, K., and Kobayashi, Y. (1995) *O*-linked oligosaccharide on IgA1 hinge region in IgA nephropathy. Fundamental study for precise structure and possible role. *Contrib. Nephrol. 111*, 73–84.
30. Novak, J., Julian, B. A., Tomana, M., and Mestecky, J. (2001) Progress in molecular and genetic studies of IgA nephropathy. *J. Clin. Immunol. 21*, 310–327.
31. Julian, B. A., and Novak, J. (2004) IgA nephropathy: An update. *Curr. Opin. Nephrol. Hypertens. 13*, 171–179.
32. Smith, A. C., and Feehally, J. (2003) New insights into the pathogenesis of IgA nephropathy. Pathogenesis of IgA nephropathy. *Springer Semin. Immunopathol. 24*, 477–493.
33. Suzuki, H., Moldoveanu, Z., Hall, S., Brown, R., Julian, B. A., Wyatt, R. J., Tomana, M., Tomino, Y., Novak, J., and Mestecky, J. (2007) IgA nephropathy: Characterization of IgG antibodies specific for galactose-deficient IgA1. *Contrib. Nephrol. 157*, 129–133.
34. Kokubo, T., Hiki, Y., Iwase, H., Horii, A., Tanaka, A., Nishikido, J., Hotta, K., and Kobayashi, Y. (1997) Evidence for involvement of IgA1 hinge glycopeptide in the IgA1-IgA1 interaction in IgA nephropathy. *J. Am. Soc. Nephrol. 8*, 915–919.
35. Mestecky, J., Tomana, M., Moldoveanu, Z., Julian, B. A., Suzuki, H., Matousovic, K., Renfrow, M. B., Novak, L., Wyatt, R. J., and Novak, J. (2008) Role of aberrant glycosylation of IgA1 molecules in the pathogenesis of IgA nephropathy. *Kidney Blood Pressure Res. 31*, 29–37.
36. Yan, Y., Xu, L. X., Zhang, J. J., Zhang, Y., and Zhao, M. H. (2006) Self-aggregated deglycosylated IgA1 with or without IgG were associated with the development of IgA nephropathy. *Clin. Exp. Immunol. 144*, 17–24.
37. Suzuki, H., Fan, R., Zhang, Z., Brown, R., Hall, S., Julian, B. A., Chatham, W. W., Suzuki, Y., Wyatt, R. J., Moldoveanu, Z., Lee, J. Y., Robinson, J., Tomana, M., Tomino, Y., Mestecky, J., and Novak, J. (2009) Aberrantly glycosylated IgA1 in IgA nephropathy patients is recognized by IgG antibodies with restricted heterogeneity. *J. Clin. Invest. 119*, 1668–1677.
38. Hiemstra, P. S., Biewenga, J., Gorter, A., Stuurman, M. E., Faber, A., van Es, L. A., and Daha, M. R. (1988) Activation of complement by human serum IgA, secretory IgA and IgA1 fragments. *Mol. Immunol. 25*, 527–533.
39. Zhang, W., and Lachmann, P. J. (1994) Glycosylation of IgA is required for optimal activation of the alternative complement pathway by immune complexes. *Immunology 81*, 137–141.
40. Roos, A., Rastaldi, M. P., Calvaresi, N., Oortwijn, B. D., Schlagwein, N., van Gijlswijk-Janssen, D. J., Stahl, G. L., Matsushita, M., Fujita, T., van Kooten, C., and Daha, M. R. (2006) Glomerular activation of the lectin pathway of complement in IgA nephropathy is associated with more severe renal disease. *J. Am. Soc. Nephrol. 17*, 1724–1734.
41. Roos, A., Bouwman, L. H., van Gijlswijk-Janssen, D. J., Faber-Krol, M. C., Stahl, G. L., and Daha, M. R. (2001) Human IgA activates the complement system via the mannan-binding lectin pathway. *J. Immunol. 167*, 2861–2868.
42. Mody, R., Joshi, S., and Chaney, W. (1995) Use of lectins as diagnostic and therapeutic tools for cancer. *J. Pharmacol. Toxicol. Methods 33*, 1–10.
43. Brooks, S. A. (2000) The involvement of *Helix pomatia* lectin (HPA) binding *N*-acetylgalactosamine glycans in cancer progression. *Histol. Histopathol. 15*, 143–158.
44. Tomana, M. (1996) in Glycoproteins and Disease (Schachter, H., Ed.) pp 291−298, Elsevier, New York.
45. Mackiewicz, A., and Mackiewicz, K. (1995) Glycoforms of serum α1-acid glycoprotein as markers of inflammation and cancer. *Glycoconjugate J. 12*, 241–247.
46. Malhotra, R., Wormald, M. R., Rudd, P. M., Fischer, P. B., Dwek, R. A., and Sim, R. B. (1995) Glycosylation changes of IgG associated with rheumatoid arthritis can activate complement via the mannose-binding protein. *Nat. Med. 1*, 237–243.
47. Ezaki, T., Baluk, P., Thurston, G., La Barbara, A., Woo, C., and McDonald, D. M. (2001) Time course of endothelial cell proliferation and microvascular remodeling in chronic inflammation. *Am. J. Pathol. 158*, 2043–2055.
48. Moore, J. S., Kulhavy, R., Tomana, M., Moldoveanu, Z., Suzuki, H., Brown, R., Hall, S., Kilian, M., Poulsen, K., Mestecky, J., Julian, B. A., and Novak, J. (2007) Reactivities of *N*-acetylgalactosamine-specific lectins with human IgA1 proteins. *Mol. Immunol. 44*, 2598–2604.
49. Moore, J. S., Wu, X., Kulhavy, R., Tomana, M., Novak, J., Moldoveanu, Z., Brown, R., Goepfert, P. A., and Mestecky, J. (2005) Increased levels of galactose-deficient IgG in sera of HIV-1-infected individuals. *AIDS 19*, 381–389.
50. Matousovic, K., Novak, J., Yanagihara, T., Tomana, M., Moldoveanu, Z., Kulhavy, R., Julian, B. A., Konecny, K., and Mestecky, J. (2006) IgA-containing immune complexes in the urine of IgA nephropathy patients. *Nephrol., Dial., Transplant. 21*, 2478–2484.
51. Sanchez, J. F., Lescar, J., Chazalet, V., Audfray, A., Gagnon, J., Alvarez, R., Breton, C., Imberty, A., and Mitchell, E. P. (2006) Biochemical and structural analysis of *Helix pomatia* agglutinin. A hexameric lectin with a novel fold. *J. Biol. Chem. 281*, 20171–20180.
52. Novak, J., Moldoveanu, Z., Renfrow, M. B., Yanagihara, T., Suzuki, H., Raska, M., Hall, S., Brown, R., Huang, W. Q., Goepfert, A., Kilian, M., Poulsen, K., Tomana, M., Wyatt, R. J., Julian, B. A., and Mestecky, J. (2007) IgA nephropathy and Henoch-Schoenlein purpura nephritis: Aberrant glycosylation of IgA1, formation of IgA1-containing immune

complexes, and activation of mesangial cells. *Contrib. Nephrol. 157*, 134–138.
53. Schuck, P. (2000) Size-distribution analysis of macromolecules by sedimentation velocity ultracentrifugation and Lamm equation modeling. *Biophys. J. 78*, 1606–1619.
54. Laue, T. M., Shah, B. D., Ridgeway, T. M., and Pelletier, S. M. (1992) in Analytical ultracentrifugation in biochemistry and polymer science (Harding, S. E., Rowe, A. J., and Horton, J. C., Eds.) pp 90−125, Royal Society of Chemistry, London.
55. Herr, A. B., White, C. L., Milburn, C., Wu, C., and Bjorkman, P. J. (2003) Bivalent binding of IgA1 to FcαRI suggests a mechanism for cytokine activation of IgA phagocytosis. *J. Mol. Biol. 327*, 645–657.
56. Herr, A. B., Ornitz, D. M., Sasisekharan, R., Venkataraman, G., and Waksman, G. (1997) Heparin-induced self-association of fibroblast growth factor-2. Evidence for two oligomerization processes. *J. Biol. Chem. 272*, 16382–16389.
57. Andre, P. M., Le Pogamp, P., and Chevet, D. (1990) Impairment of jacalin binding to serum IgA in IgA nephropathy. *J. Clin. Lab. Anal. 4*, 115–119.
58. Hiki, Y., Odani, H., Takahashi, M., Yasuda, Y., Nishimoto, A., Iwase, H., Shinzato, T., Kobayashi, Y., and Maeda, K. (2001) Mass spectrometry proves under-*O*-glycosylation of glomerular IgA1 in IgA nephropathy. *Kidney Int. 59*, 1077–1085.
59. Lee, R. T., and Lee, Y. C. (2000) Affinity enhancement by multivalent lectin-carbohydrate interaction. *Glycoconjugate J. 17*, 543–551.
60. Tachibana, K., Nakamura, S., Wang, H., Iwasaki, H., Maebara, K., Cheng, L., Hirabayashi, J., and Narimatsu, H. (2006) Elucidation of binding specificity of Jacalin toward *O*-glycosylated peptides: Quantitative analysis by frontal affinity chromatography. *Glycobiology 16*, 46–53.
61. Allen, A. C., Bailey, E. M., Barratt, J., Buck, K. S., and Feehally, J. (1999) Analysis of IgA1 *O*-glycans in IgA nephropathy by fluorophore-assisted carbohydrate electrophoresis. *J. Am. Soc. Nephrol. 10*, 1763–1771.
62. Hiki, Y., Tanaka, A., Kokubo, T., Iwase, H., Nishikido, J., Hotta, K., and Kobayashi, Y. (1998) Analyses of IgA1 hinge glycopeptides in IgA nephropathy by matrix-assisted laser desorption/ionization time-of-flight mass spectrometry. *J. Am. Soc. Nephrol. 9*, 577–582.
63. Shimozato, S., Hiki, Y., Odani, H., Takahashi, K., Yamamoto, K., and Sugiyama, S. (2008) Serum under-galactosylated IgA1 is increased in Japanese patients with IgA nephropathy. *Nephrol., Dial., Transplant. 23*, 1931–1939.
64. Boehm, M. K., Woof, J. M., Kerr, M. A., and Perkins, S. J. (1999) The Fab and Fc fragments of IgA1 exhibit a different arrangement from that in IgG: A study by X-ray and neutron solution scattering and homology modelling. *J. Mol. Biol. 286*, 1421–1447.